Radboud Repository

Radboud University Nijmegen

PDF hosted at the Radboud Repository of the Radboud University Nijmegen

The following full text is a publisher's version.

For additional information about this publication click this link.
http://hdl.handle.net/2066/23921

Please be advised that this information was generated on 2017-12-05 and may be subject to change.

Journal of Orthopaedic Research
14:36-43 The Journal of Bone and Joint Surgery, Inc.
© 1996 Orthopaedic Research Society

Friction and Stem Stiffness Affect Dynamic Interface Motion in Total Hip Replacement

Jan Herman Kuiper and Rik Huiskes

Biomechanics Section, Institute of Orthopaedics, University of Nijmegen, Nijmegen, The Netherlands

Summary: Large cyclic movements between the femoral stem and bone during the first weeks after total hip arthroplasty may hamper bone ingrowth and adversely affect the eventual success of the arthroplasty. Little is known, however, about the magnitude of the motions and its relationship to design and surgical factors. A two-dimensional finite element model of a cementless prosthesis inserted into the proximal femur was constructed to study the effects of two mechanical variables—the stiffness of the implant and the coefficient of friction between bone and implant—on the magnitude of the motions. We investigated the influences of these variables on the subsidence of the prosthesis, the magnitudes of the cyclic motions, and the level of the interface stresses. The presence of friction reduced cyclic motions by about 85% compared with a frictionless interface. Once friction was assumed, varying the coefficient of friction had little effect. The effect of friction on the interface stress state and gross subsidence of the prosthesis was not as great as on cyclic motion. Implant stiffness also affected the magnitudes and distributions of the cyclic motions along the interface. A flexible stem generated motions about three to four times larger proximally than those of a stiff stem, which generated larger motions distally. The influence of stem stiffness on interface stresses and prosthetic subsidence was less than on cyclic motion. The location of the peak shear stresses at the interface around a bonded prosthesis corresponded to the location where cyclic interface motion was maximal for an unbonded prosthesis. However, no direct relationship was found between the magnitudes of peak stresses and the amplitudes of cyclic motions.

Following implantation, cementless implants are not bonded to the surrounding bone. Loading the prosthesis therefore causes movements of the prosthesis relative to the bone. These motions at the bone-implant interface have a notable effect on the clinical success of cementless hip arthroplasty. For porous-coated devices, the amplitudes of the micromotions determine whether bone grows into or apposes the coated surface and whether the implant is encapsulated by a layer of fibrous tissue (12,19,20). For press fit devices, the amplitudes of the motions probably determine whether or not a stable interface develops and is maintained (14,21).

Laboratory experiments, performed to assess the amplitudes of the motions, have revealed differences between the "initial stability" (the immediate postoperative resistance to motions at the interface) of various cementless prosthetic designs (1,8,11,16,17). However, they revealed little about the mechanisms that govern the movements. For instance, the relationship between stresses at the interface, frictional properties of the bone-prosthesis connection, and relative motions is unknown. The present study explored the use of the finite element method as a tool to investigate the mechanisms that govern motions as the result of a continuous loading cycle. We studied two aspects: the influence of friction at the bone-implant interface and the influence of implant stiffness. In addition, we evaluated how friction at the interface influenced the mechanism of load transfer from an unbonded prosthesis to the surrounding bone in comparison with a frictionless unbonded interface and with a fully bonded interface.

Received August 13, 1993; accepted May 31, 1995.

Address correspondence and reprint requests to R. Huiskes at Biomechanics Section, Institute of Orthopaedics, University of Nijmegen, P.O. Box 9101, 6500 HB Nijmegen, The Netherlands.

Presented in part at the 39th annual meeting of the Orthopaedic Research Society in San Francisco, California, U.S.A, February 17, 1993.

METHODS

A two-dimensional finite element model of the proximal femur with a precisely fitting collarless implant was constructed using four-node linear plain-strain elements (Fig. 1). The femur consisted of cortical bone with a Young's modulus (E) of 17 GPa and cancellous bone with a Young's modulus of 0.6 GPa. A side-plate with the properties of cortical bone was added to account for the three-dimensional structural integrity of the bone. Contact between prosthesis and bone was represented by gap elements that employed Lagrange nodes to enforce the contact conditions. The MARC finite element program (MARC Analysis, Palo Alto, CA, U.S.A.) was used to solve the finite element model equations. A set of three joint loading cases, representing normal daily activities (2), was applied in a dynamic loading cycle (Fig. 1). Loading case 1 (2,317 N at 24° of flexion) represented the hip joint load during

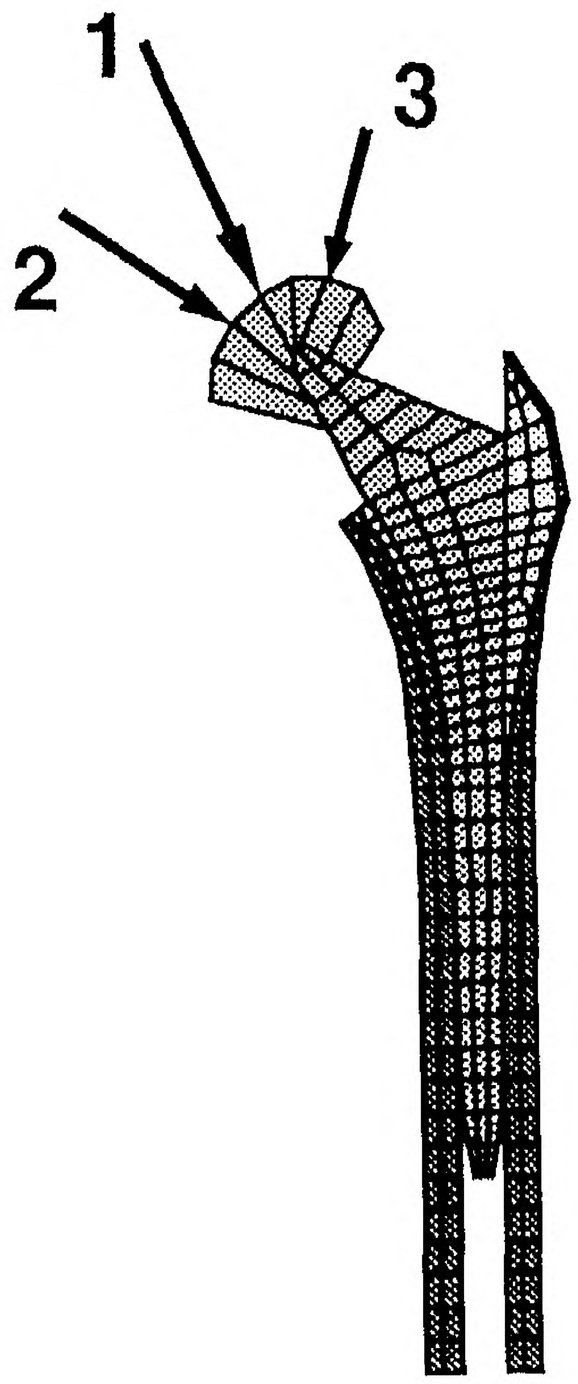

FIG. 1. Two-dimensional finite element model of a bone-prosthesis configuration. A side-plate connects the medial and lateral cortices. The three loading cases are shown.

the stance phase of walking; loading cases 2 (1,548 N at 56° of flexion) and 3 (1,158 N at 15° of retroflexion) represented more extreme daily loads that occur less frequently. The dynamic loading cycle consisted of the three loading cases applied sequentially (1, 2, 1, 3, 1, 2, and so on). The transition from one loading case to the next was accomplished in five time steps, the minimal number for not compromising convergence or accuracy. For each loading case, convergence was assumed when the maximal deviation from equilibrium of the internal nodal forces was less than 1% of the maximal nodal reaction force.

Three different values for the coefficient of friction (μ) between bone and prosthesis were studied: $\mu = 0.0$ (no friction), $\mu = 0.15$ (lubricated friction), and $\mu = 0.40$ (unlubricated friction). The second value is a typical one in the presence of a "fairly effective" lubricant (10); it was assumed that a mixture of blood and marrow acts as such. The third value ($\mu = 0.40$) is a typical one for unlubricated or poorly lubricated friction between metals and nonmetals (10) and corresponds to experimentally determined coefficients of friction between wet bone and smooth titanium (4,18). For comparison, the same prosthesis was studied with the assumption that it was fully bonded to the surrounding bone. Two different values for the Young's modulus of the prosthetic material were investigated: $E = 110$ GPa (titanium alloy) and $E = 17$ GPa (a hypothetical isoelastic material with the same modulus as cortical bone).

For each value of parameters μ and E, we determined the gross subsidence of the prosthetic tip, the amplitude of the relative motions at the interface, and the interface stresses. Subsidence was defined as the total displacement between the prosthetic tip and the adjacent bone, averaged over one loading cycle; thus, it was the "rigid-body" displacement of the prosthesis relative to the bone. The amplitudes of the interface motions were defined as the amplitudes of the difference in maximal displacements between prosthesis and bone at the interface within one full loading cycle. In addition, we determined the amplitudes of the gross motions, which were the amplitudes of the differences in cyclic displacement between the proximal lateral side of the prosthesis and the top of the greater trochanter, during one loading cycle. This quantity has often been measured in laboratory experiments to assess the amplitude of the interface motions (8,17).

The interface stresses were separated into a component perpendicular to the prosthetic surface (normal stress) and a component parallel to the prosthetic surface (shear stress). We calculated the interface stresses at each gap node by dividing the gap force (in normal and shear directions, respectively) by the area of the element sides attributed to the gap node.

RESULTS

The presence or absence of friction at the interface substantially influenced the general behavior of the model. When frictionless interface contact was assumed, each new loading cycle generated the same displacements as the previous one. During the loading cycle, the prosthesis was moved up and down inside the bone, like a rigid body (Fig. 2). When friction was assumed, the behavior changed. Instead of moving the prosthesis up and down, as in the frictionless case, each new loading cycle gradually drove the prosthesis further into the bone, until (after five to eight cycles) a steady state was reached (Fig. 2). At the steady state, each new loading cycle led to a repetition of the prosthetic motion of the previous cycle. Within a loading cycle, the differences in displacement of the prosthetic tip relative to the bone hardly varied, although at the interface the prosthesis still moved relative to the bone.

Regardless of the coefficient of friction, the isoelastic stem migrated more than the titanium stem, although the differences were not extensive (Fig. 3). When lubricated friction was assumed ($\mu = 0.15$), the average steady-state subsidence was slightly greater than the value found for frictionless contact. However, the peak subsidence (the sum of the average subsidence and cyclic movement) was less. For unlubricated friction ($\mu = 0.40$), the average subsidence

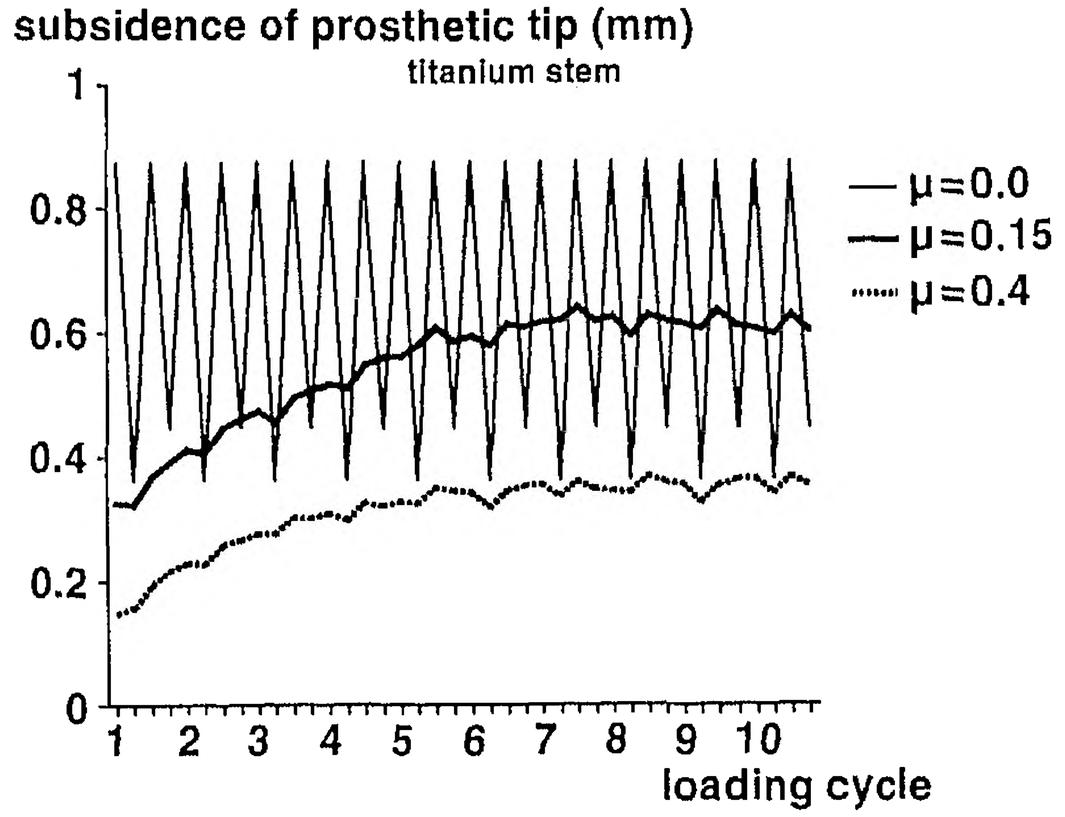

FIG. 2. Subsidence of the stem tip during the first eight loading cycles for a titanium prosthesis, assuming three different values for the coefficient of friction (μ) at the interface.

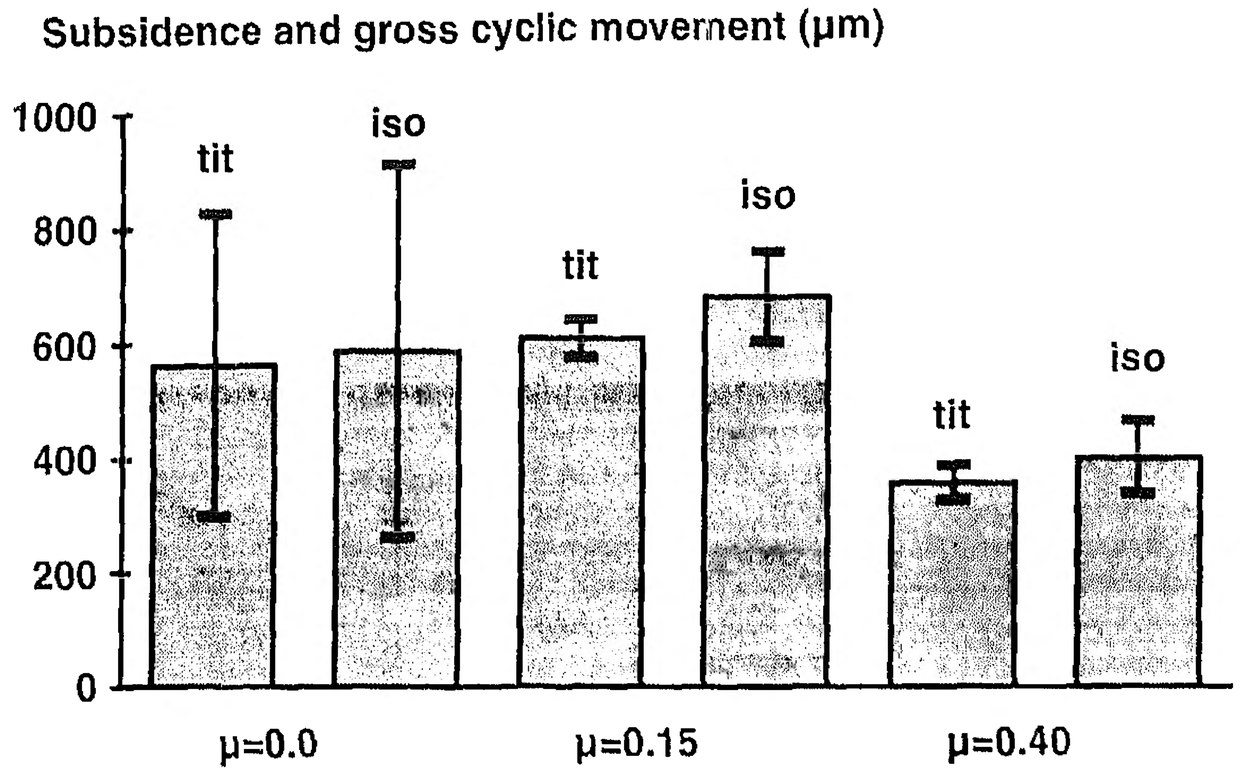

FIG. 3. Average subsidence of the stem tip (gray bar) and amplitude of gross cyclic movements (I) in the steady state for two values o. the prosthetic Young's modulus (equivalent to titanium [tit] and isoelastic [iso]) and three values of the coefficient of friction (µ) betweer bone and implant.

was clearly less than that of either of the other cases.

The influences of friction and Young's modulus on the steady-state amplitude of the interface motions were much larger than on the subsidences. Both the values and the distributions of the amplitudes along the interface were affected. Without friction, the amplitudes of the interface motions were uniformly distributed (Fig. 4). Although the isoelastic stem generated somewhat larger motions, the differences between the types of prostheses were relatively small. When friction was introduced, the amplitudes of the motions were reduced considerably. Even assuming little friction ($\mu = 0.15$), the reduction was at least 65% (at the medial-proximal interface of the isoelastic stem) and averaged 85%. In addition, considerable differences between the stems in the distribution of motions occurred. Around the titanium stem, the larger amplitudes took place distally, whereas around the isoelastic stem the larger amplitudes occurred proximally. Regardless of the type of friction assumed (lubricated or unlubricated), the largest motion occurred at the proximal-medial interface of the isoelastic stem. Its amplitude was 150-200 µm, which was three to four times the amplitude found around the titanium stem. The smallest interface motions occurred at the proximal-lateral interface of the titanium stem, where the amplitudes (2-20 µm) were about one-third of the values found elsewhere. The amplitude of the gross motion between the proximal prosthetic surface and the top of the greater trochanter was in the

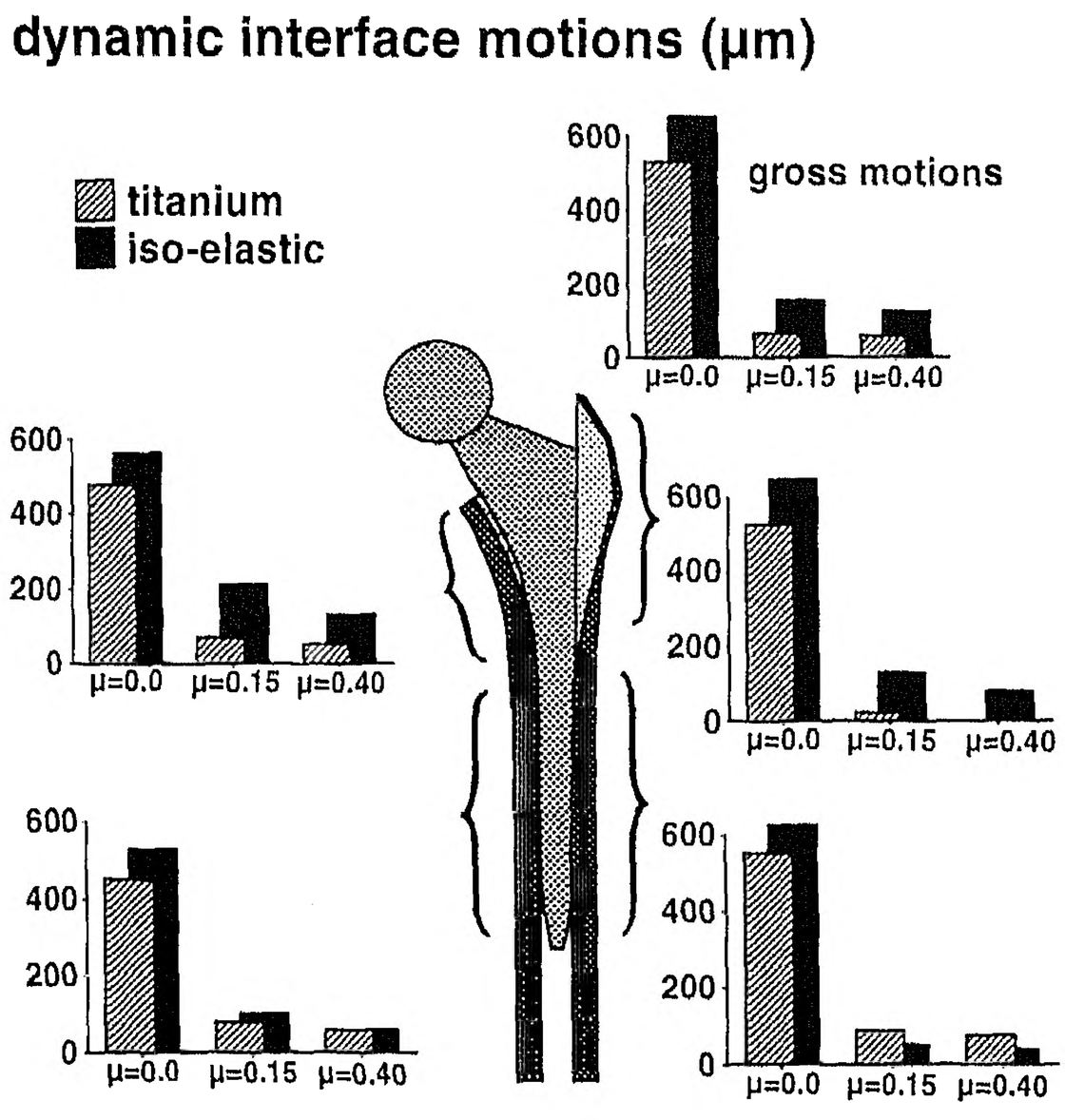

FIG. 4. Amplitudes of the cyclic interface motions along the interface in the steady state for two values of the prosthetic Young's modulus and three values of the coefficient of friction (µ) between bone and implant.

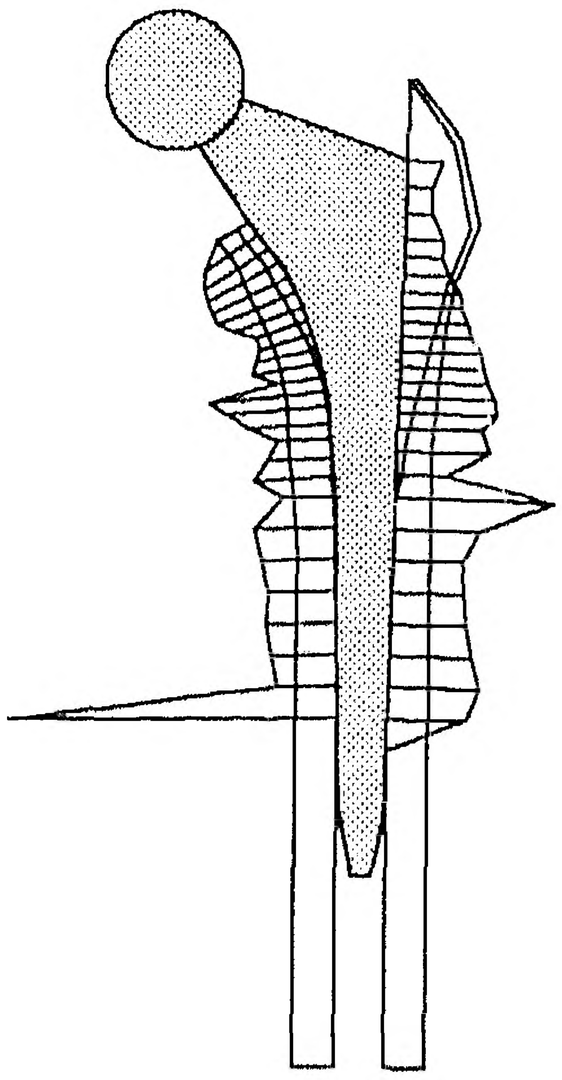

FIG. 5. Distribution of the interface normal stress in the steady state around a titanium prosthesis that is loaded according to loading case 1, assuming a coefficient of friction of $\mu = 0.15$ between bone and implant.

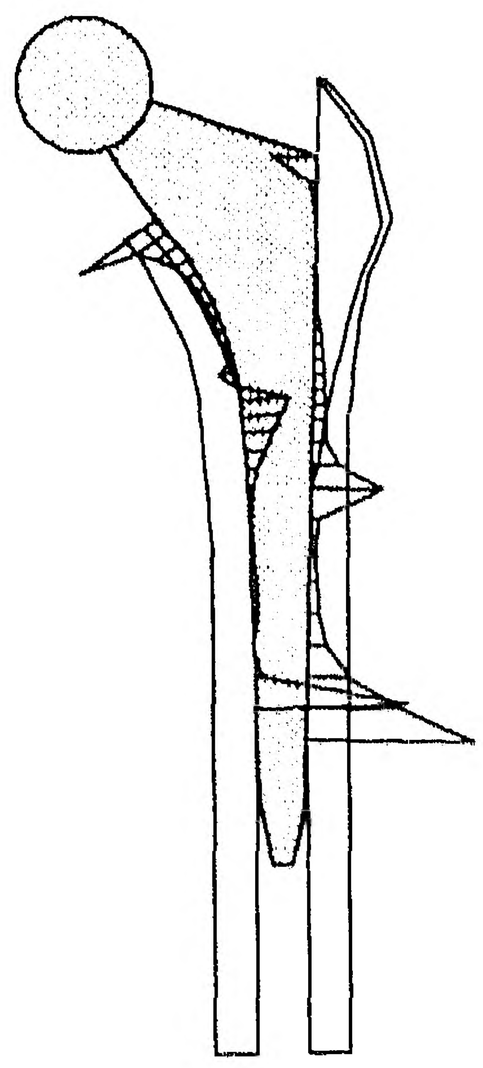

FIG. 6. Distribution of the interface normal stress in the steady state around a fully bonded titanium prosthesis that is loaded according to loading case 1.

range of the average amplitude of the interface motions (Fig. 4). The general effects of stem flexibility and frictional properties on the gross motion were the same as on the interface motions.

Regardless of prosthetic stiffness, frictional coefficient, or loading case, a similar pattern of interface normal stresses around the unbonded prosthesis was always found (Fig. 5). Large compressive stresses were uniformly distributed along the stem, except for a distinct peak distally, smaller peaks at the transition region of cortical and cancellous bone, and a slight drop at the proximal lateral side. Because the shear stresses were linearly related to the normal stresses through the coefficient of friction, they followed a similar pattern. During the dynamic loading cycle, the orientation of the shear stresses continuously reversed, depending on the direction of the relative movements at the interface. The distribution of interface normal stress around a bonded stem showed a clearly different pattern when compared with that around an unbonded stem (Fig. 6). Except for distinct peaks proximally and laterally and at the transition of cortical and cancellous bone, the interface normal stresses around the bonded stems were relatively low.

For all three values of the coefficient of friction, as well as for the bonded stem, the isoelastic prosthesis generated larger proximal interface stresses, whereas the titanium prosthesis generated larger distal stresses (Figs. 7 and 8). Hence, the interface stresses revealed the same trend as the interface motions. The difference between the two stem types was most clear in the distributions of interface shear stress around the bonded stems. The relative differences between these stress components were of the same order of magnitude as the differences in cyclic interface motions, except for the distal medial side (Fig. 4 compared with Fig. 8).

An increase in the coefficient of friction reduced the interface normal stresses around the unbonded prosthesis (Fig. 7), simultaneously elevating the interface shear stresses (Fig. 8). Comparison of the interface normal stresses for frictionless and lubricated contact ($\mu = 0.0$ compared with $\mu = 0.15$) revealed a difference of 30% at most; this suggests that the effect of a small amount of friction on the distribution of interface stress was much less than on the amplitudes of the interface motions, where a difference of at least 65% was found. Changing the interface condition from unbonded to bonded had a notable influence on magnitudes of stress.

DISCUSSION

The prevalent motions of a prosthesis relative to the bone occur in the direction of the longitudinal axis (subsidence) and around the longitudinal axis (rotation). Studies from the past few years (1,11,16) have suggested that rotational motion may be the most important clinically. An accurate, simultaneous analytical simulation of both axial and rotational motion components requires a three-dimensional finite element model (7,13). In this study, we used a two-dimensional side-plated model. Our results were therefore confined to movements in the longitudinal direction. However, the principal goal of this study was not the accurate simulation of all relevant motions. Instead, the emphasis was on understanding the effects of friction and prosthetic stiffness on the relative motions

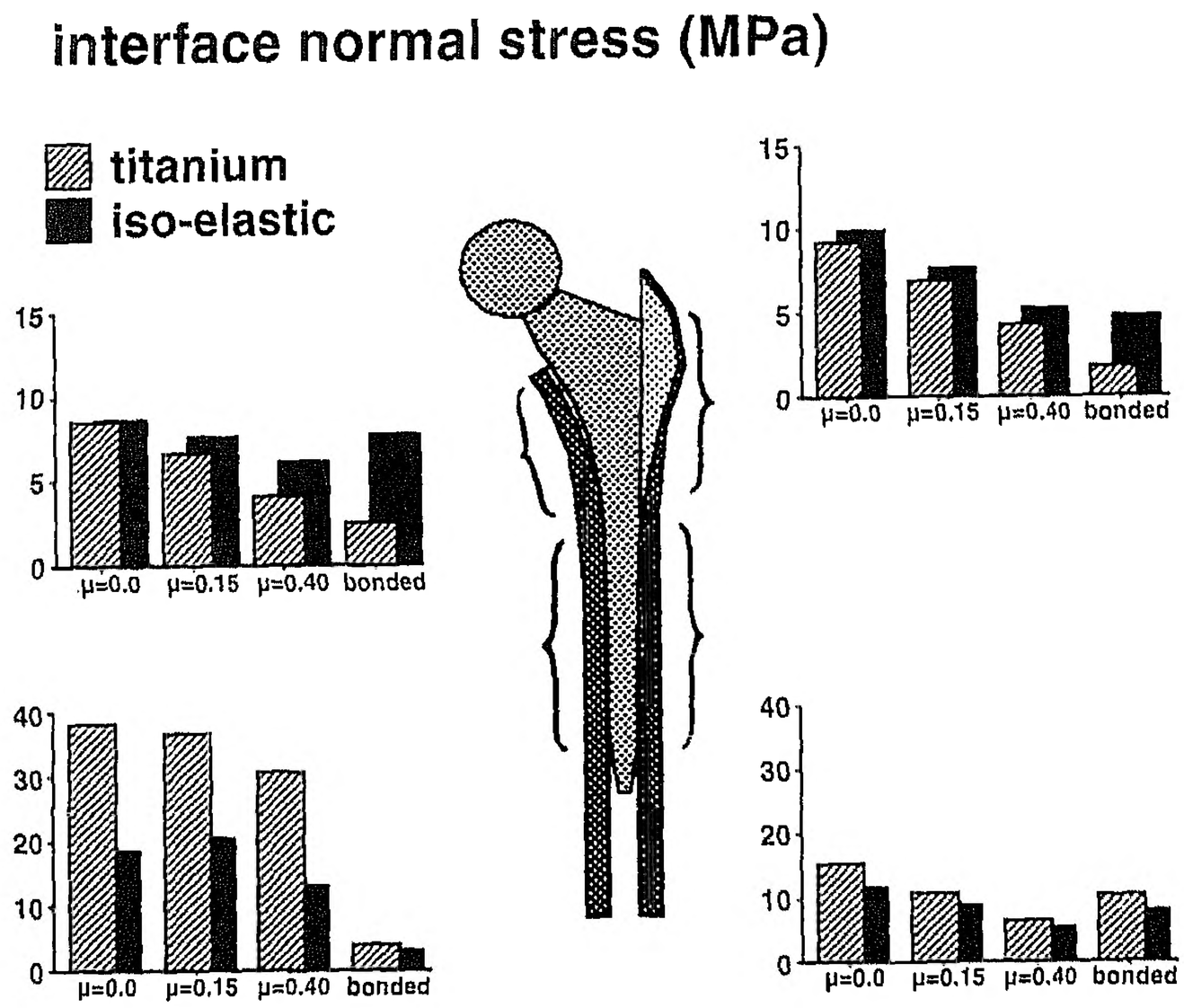

FIG. 7. Distribution of the interface normal stress in the steady state around an unbonded stem, using three different values of th coefficient of friction (μ) between bone and implant, and around a fully bonded stem. Two values for the prosthetic stiffness were usec

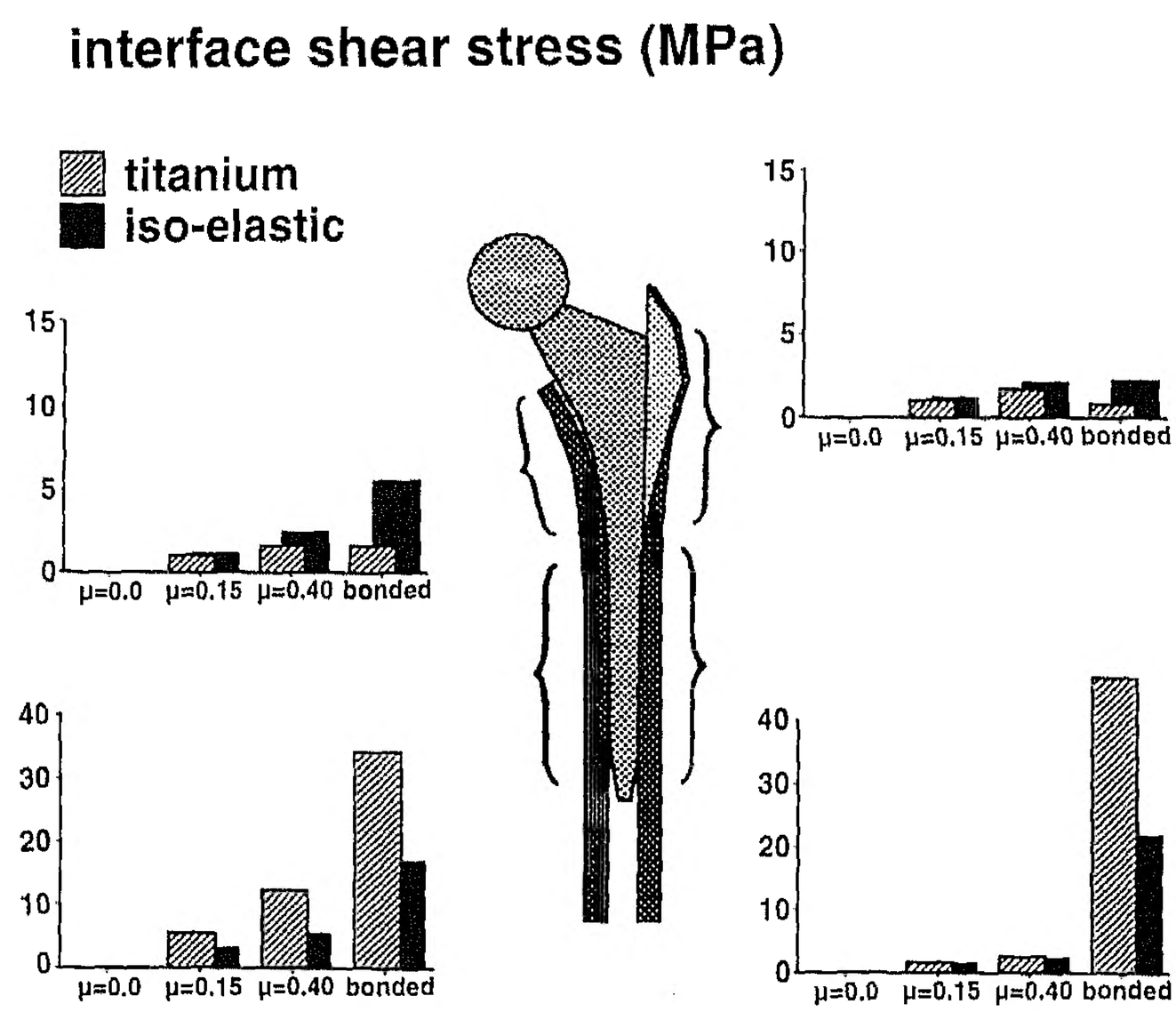

FIG. 8. Distribution of the interface shear stress in the steady state around an unbonded stem, using three different values of the coefficient of friction (μ) between bone and implant, and around a fully bonded stem. Two values for the prosthetic stiffness were used.

and the load transfer at the bone-implant interface under the influence of a continuous loading cycle. The adequacy of a similar two-dimensional model was examined by Verdonschot and Huiskes (22). Assuming fully bonded or frictionless interface contact, they compared the interface stresses as obtained from a two-dimensional model with those obtained from three-dimensional models. As long as the loading was restricted to the midfrontal plane, satisfactory qualitative and quantitative agreement was found.

The assumed dynamic loading cycle was not meant to represent a particular physiological activity such as walking or stair climbing. Rather, it was a combination of the hip joint load during the stance phase of walking (loading case 1) and two extreme loading cases that might occur (2). Hence, the loading cycle represented an envelope of possible daily loading, so that the calculated relative displacements may be regarded as the maximal daily displacements. Of course, other loading cycles are conceivable, such as one simulating walking. Although choosing another loading cycle would certainly affect the results that were found,

it would not significantly influence the mechanisms.

We ignored the influence of abductor loads in our analysis. Including them would have increased the bending load in the model and, since most of the motion in our model was probably caused by bending, the magnitudes of the motions would have increased. However, we do not think that incorporating abductor forces would have influenced our results in a qualitative sense.

Bearing these assumptions and limitations in mind, the emphasis must be on conceptual, qualitative aspects of the results, and the reported values from this study should be extrapolated to clinical cases with great caution. We were interested only in the effects of friction and stem stiffness and did not address prosthetic design (e.g., collared compared with collarless), prosthetic loading, bone quality, and interface conditions (e.g., proximally coated compared with fully coated) that could influence results.

We can compare the results of our model with those obtained from laboratory experiments in which a dynamic loading cycle was applied (8,16,17). The general mechanism of a gradual increase of prosthetic subsidence toward a steady state, found when interface friction was assumed, was also observed experimentally. When a frictionless interface was assumed, the analytical results deviated from experimental results and were therefore less realistic. The amount of gross prosthetic subsidence reached at a steady state is difficult to compare quantitatively, even when loading cases, geometries, and materials correspond. In our study, we assumed a precise initial fit between prosthesis and bone. Hence, in the model, subsidence was primarily caused by straining of the side-plate, which represented straining of the bone in the circumferential direction. It is impossible to prepare a precise fit experimentally (9,15), even when using a synthetic femur (8). For this reason, subsidence in the experiments was not only caused by straining bone but also by "seating" of the implant, in which local "gaps" between bone and implant are closed by impacting the bone. Our results suggest, however, that the initial transient subsidence found experimentally was not due exclusively to seating but that frictional effects played an important role as well.

The amplitudes of the cyclic interface motions in the steady state may be less sensitive to the seating mechanism. In addition, their relevance to clinical performance is probably larger since it is the cyclic motion, rather than the total subsidence, that compromises clinical success by hampering ingrowth and inducing formation of fibrous tissue (12,14,19-21). Because the actual relative motions at the interface could not be determined in experimental models, we determined the amplitudes of the gross motions, which were the amplitudes of the cyclic motion of the proximal side of the prosthesis relative to the greater trochanter. The titanium stem generated gross-motion amplitudes of 59-66 μm when friction was assumed and of about 500 μm when a frictionless interface was assumed. In experiments, McKellop et al. (8) measured values of 20-50 μm and Sharkey et al. (17) measured values of 10-110 μm, on the same order as the analytical results with the assumption of friction. The correspondence between the values suggests that the choice of interface friction is more appropriate than a frictionless interface.

Konieczynski and Bartel (7) and Rubin and coworkers (13), using three-dimensional finite element models, found relative displacements of 300-500 μm at the interface. They did not apply a dynamic loading cycle, however, and therefore could not distinguish between subsidence and cyclic motions. The difference in axial displacement of about 300 μm at the stem tip agrees with the range of the subsidence of the stem tip after the first loading cycle (Fig. 3); this suggests that for corresponding cases, our simplified model showed behavior similar to their more elaborate models. Our results suggest that the values of displacement difference calculated in these three-dimensional models relate to a transient state rather than to a steady state and therefore may have little significance to clinical performance.

An advantage of finite element modeling, as compared with experiments, is the ability to determine the relative motions between prosthesis and bone at the location where they matter: the bone-implant interface. The amplitude distribution of the interface motions revealed details that would not have been appreciated if only the gross amplitudes were considered. For the stiffer titanium prosthesis, the amplitude of the interface motions at the proximal-lateral interface was less than at other parts of the interface. Assuming that smaller motions facilitate bone growth into a coated stem, the results suggest that bone ingrowth will occur initially at the proximal-lateral interface. Studies of early retrieved prostheses seem to support this hypothesis (3). The small proximal lateral amplitude was probably caused by the large bulk of flexible cancellous bone inside the greater trochanter, adjacent to the proximal-lateral interface. This bone acted as a cushion between cortical bone and prosthesis, and its deformations bridged the difference in displacement between cortical bone and titanium prosthesis. The same cushioning effect did not occur around the flexible implant, where the gross motion was about three times larger than for the stiff prosthesis.

The relatively large proximal motions that are generated by the flexible implant may prevent bone ingrowth into coatings. When ingrowth fails, or when a coating is not present, the prosthesis will function as a

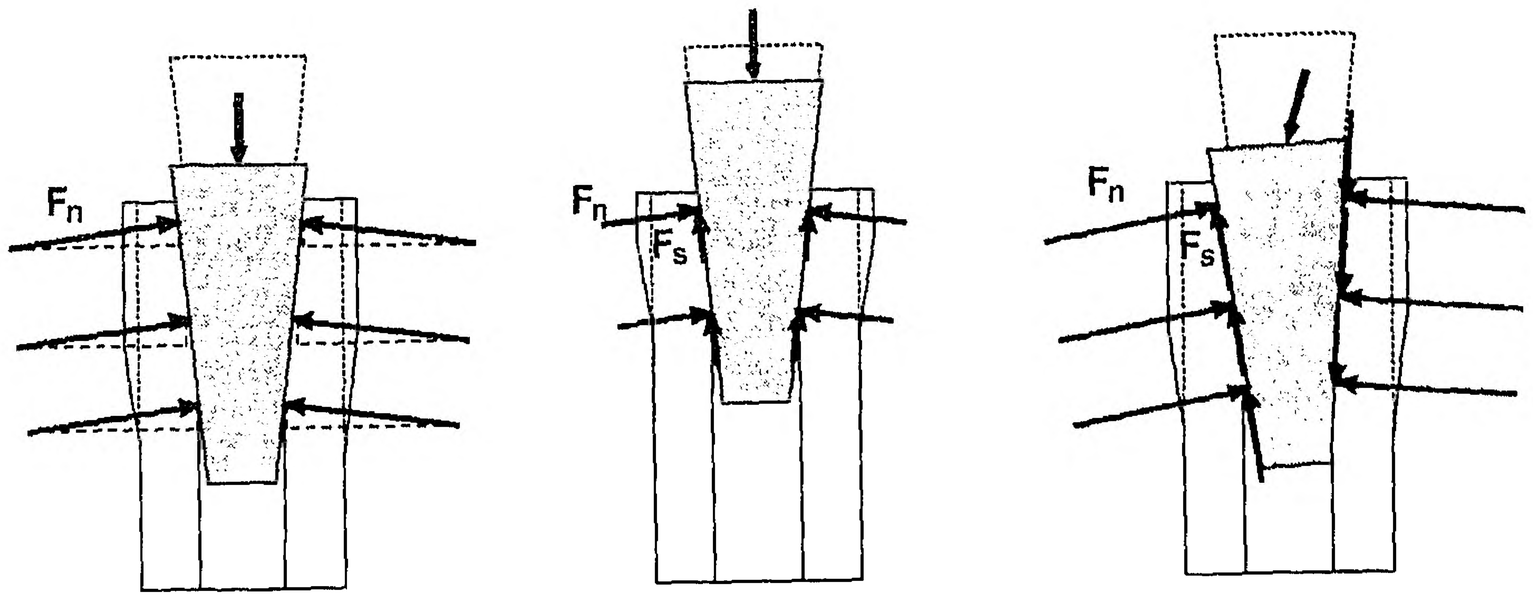

FIG. 9. Schematic representation of the distribution of interface stress around a straight taper. **a:** No friction between bone and taper is assumed. The taper is supported only by the vertical component of the interface normal stress (F_n). **b:** Friction between bone and taper is assumed. The taper is supported by the summed vertical components of the interface normal stress and the interface shear stress (F_s). **c:** The effect of a tilting load. The load tends to rotate the taper. As a consequence, the interface movements at both sides will have an opposite direction, and the interface shear stresses will be in opposite directions. The net axial reaction force, which is the sum of the sum of the vertical components of interface normal and shear stresses, is therefore less, and the taper will be driven further into the bone.

press fit implant, surrounded by a layer of fibrous tissue (20). Such a layer ensures a very low coefficient of friction. When a low coefficient of friction ($\mu = 0.15$) was assumed, however, the cyclic interface motions around the flexible implant were still substantially larger than those around the stiff implant. These results suggest that the clinical performance of a press fit flexible implant will be inferior to that of a press fit stiff implant. Otani et al. (11) reached the same conclusion from laboratory experiments. The difference in interface motion amplitude may partly explain the high early failure rate of the isoelastic RM prosthesis, as compared with stiffer designs (6).

Increasing the coefficient of friction from 0.0 to 0.4 reduced stem subsidence and normal interface stresses but, compared with the effects on cyclic interface motions, the influence was less pronounced. The stress patterns in the interface were not affected and remained more uniformly distributed. The relatively small effect of friction on stem subsidence and stress distribution in the interface was due to the inclusion of a dynamic loading cycle. Conceptually, an unbonded prosthesis can be considered as a taper placed inside a ring of bone (5). When loaded axially, the taper sinks into the bone, thereby straining the bone circumferentially and generating interface stresses (Fig. 9). Without friction, no shear stresses are possible, and the axial load on the taper must be balanced by the vertical component of the interface normal stresses (Fig. 9a). These normal stresses are caused by the straining of the bone and hence depend on the subsidence of the taper. When interface friction is present, interface shear stresses are generated that are linearly related to the normal stresses through the coefficient of friction. These shear stresses contribute significantly to balancing the axial load, in particular when the taper angle is small (Fig. 9b). As a consequence, smaller interface normal stresses are required, and the taper subsidence is less. However, the orientation of the shear stress depends on the direction of the relative displacement between bone and prosthesis. When the taper load is allowed to vary its direction, the taper sides tend to move in an opposite direction. As a consequence, the interface shear stresses have an opposite orientation and therefore contribute less to balancing the taper load (Fig. 9c). Hence, a dynamic load drives the taper further into the bone than a static load does and partly compensates for the effect of friction.

Stiffness of the stem had little effect on subsidence toward the steady state and on the stress patterns in the interface around the unbonded stems. Compared with the titanium stem, the isoelastic stem migrated slightly further and generated somewhat larger proximal and smaller distal interface stresses. This difference was retained irrespective of the coefficient of friction. The larger subsidence can also be understood by the conceptual model of a taper inside a bony ring (Fig. 9). Sinking the taper into the bone causes straining of the bone and generates interface stresses. However, these stresses also compress the prosthesis. The more flexible the prosthesis, the more compression it allows and the further it sinks. As a consequence, somewhat higher proximal interface stresses are generated.

An important question is whether interface stresses around a bonded stem indicate that cyclic interface motions would occur along the same stem without bonding. The location (proximal or distal) of the highest interface peak stress around the bonded stem corresponded to the location of the largest amplitude of the cyclic interface motion around the unbonded stem; this suggests that smaller proximal or distal interface stress peaks indicate smaller proximal or distal cyclic motions at the same location. However, the largest

shear stress peaks were found at the tip of the bonded titanium stem, whereas the largest cyclic motions were found at the proximal interface of the flexible stem. It seems, therefore, that no relation exists between the location of the highest interface stress peak and the location of the largest cyclic interface motions.

On the basis of these results, we conclude that studies of relative motions of hip stems should be performed using dynamic loading cycles, in both finite element and experimental models. This is necessary to distinguish an initial transient phase from a steady-state phase. In particular, motions at the bone-implant interface are markedly influenced by the presence of interface friction, even for low friction coefficients, and this should be accounted for when analytical studies are performed. Steady-state cyclic interface motions, in the presence of friction, are quite sensitive to stem stiffness. Flexible stems provoke excessive dynamic motions, particularly on the proximal side. Finally, shear stresses at bonded stem interfaces are indicative of, but not proportional to, cyclic interface motions after debonding.

REFERENCES

1. Callaghan JJ, Fulghum CS, Glisson R, Stranne SK: The effect of femoral stem geometry on interface motion in uncemented porous-coated total hip prostheses: comparison of straight-stem and curved-stem designs. *J Bone Joint Surg [Am]* 74:839-848, 1992
2. Carter DR, Orr TE, Fyhrie DP: Relationships between loading history and femoral cancellous bone architecture. *J Biomech* 22:231-244, 1989
3. Collier JP, Mayor MB, Chae JC, Surprenant VA, Surprenant HP, Dauphinais LA: 1988 proceedings of the Hip Society—symposium: macroscopic and microscopic evidence of prosthetic fixation with porous-coated materials. *Clin Orthop* 235:173-180, 1988
4. Hayes WC, Perren SM: Plate-bone friction in the compression fixation of fractures. *Clin Orthop* 89:236-240, 1972
5. Huiskes R: The various stress patterns of press-fit, ingrown, and cemented femoral stems. *Clin Orthop* 261:27-38, 1990
6. Jakim I, Barlin C, Sweet MBE: RM isoelastic total hip arthroplasty: a review of 34 cases. *J Arthroplasty* 3:191-199, 1988
7. Konieczynski DD, Bartel DL: The effects of bone quality and interface friction on early post-operative performance of an anatomic noncemented implant. *Trans Orthop Res Soc* 18:447, 1993
8. McKellop H, Ebramzadeh E, Niederer PG, Sarmiento A: Comparison of the stability of press-fit hip prosthesis femoral stems using a synthetic model femur. *J Orthop Res* 9:297-305, 1991
9. Noble PC, Alexander JW, Maltry JA, Yew DT, Tullos HS: The myth of a press-fit cementless femoral prosthesis. Presented at the 55th Annual Meeting of The American Academy of Orthopaedic Surgeons, Atlanta, 1988
10. O'Connor JJ: *Standard Handbook of Lubrication Engineering*. New York, McGraw-Hill, 1968
11. Otani T, Whiteside LA, White SE, McCarthy DS: Effects of femoral component material properties on cementless fixation in total hip arthroplasty: a comparison study between carbon composite, titanium alloy, and stainless steel. *J Arthroplasty* 9:67-74, 1993
12. Pilliar RM, Lee JM, Maniatopoulos C: Observations on the effect of movement on bone ingrowth into porous-surfaced implants. *Clin Orthop* 208:108-113, 1986
13. Rubin PJ, Rakotomanana RL, Leyvraz PF, Zysset PK, Curnier A, Heegaard JH: Frictional interface micromotions and anisotropic stress distribution in a femoral total hip component. *J Biomech* 26:725-739, 1993
14. Schatzker J, Horne JG, Sumner-Smith G: The effect of movement on the holding power of screws in bone. *Clin Orthop* 111:257-262, 1975
15. Schimmel J-W, Huiskes R: Primary fit of the Lord cementless total hip: a geometric study in cadavers. *Acta Orthop Scand* 59:638-642, 1988
16. Schneider E, Eulenberger J, Steiner W, Wyder D, Friedman RJ, Perren SM: Experimental method for the in vitro testing of the initial stability of cementless hip prostheses. *J Biomech* 22:735-744, 1989
17. Sharkey PF, Albert TJ, Hume EL, Rothman RH, Beauchamp JA: Initial stability of femoral components in total hip arthroplasty: a comparative study. *Trans Orthop Res Soc* 16:517, 1991
18. Shirazi-Adl A, Dammak M, Forcione A, Paiement G: Friction measurements at the bone/implant interface—application to the analysis of cementless prostheses. *Trans Orthop Res Soc* 17:382, 1992
19. Søballe K, Hansen ES, Rasmussen HB, Bünger C: Hydroxyapatite implant coating modifies membrane formation during unstable mechanical conditions. *Trans Orthop Res Soc* 16:35, 1991
20. Specter M: Current concepts of bone ingrowth and remodeling. In: *Non-Cemented Total Hip Arthroplasty*, pp 69-85. Ed by RH Fitzgerald Jr. New York, Raven Press, 1988
21. Uhthoff HK, Germain J-P: The reversal of tissue differentiation around screws. *Clin Orthop* 123:248-252, 1977
22. Verdonschot N, Huiskes R: FEM analyses of hip prostheses: validity of the 2-D side plate model and the effects of torsion. In: *Proceedings of the 7th Meeting of the European Society of Biomechanics*, p A20, Århus, July 1990